

Application of the Mössbauer effect to the characterization of an amorphous tin-oxide system

G. S. Collins,* T. Kachnowski, and N. Benczer-Koller
Rutgers University, New Brunswick, New Jersey 08903

M. Pasternak
University of Tel Aviv, Ramat Aviv, Israel
(Received 14 September 1978)

Mössbauer, electron-micrography, and electron-diffraction studies were conducted on amorphous-tin-oxide samples prepared by reacting gaseous atomic tin with molecular oxygen and collecting the oxide on a 77-K substrate. The observed isomer shift, quadrupole splitting, and characteristic lattice temperatures deviate significantly from the values for crystalline SnO₂ and SnO. A qualitative description of the oxidation reaction mechanism and a proposed structure of the amorphous material are given.

INTRODUCTION

The Mössbauer effect is a unique tool for investigating structural and dynamical aspects of solids on an atomic scale. Combined measurements of the hyperfine interactions and of the recoil-free fraction and its temperature dependence provide information, not always attainable by other methods, on symmetry, ordering, and chemical bonding in the immediate vicinity of the probing nucleus. Recently, Mössbauer spectroscopy has been applied to the studies of amorphous materials.¹

The empirical description of a solid as amorphous depends on the spatial resolution of the analytic method employed. The traditional methods such as x rays, electron microscopy, and diffraction are limited to a resolution of tens of angstroms. Some crystalline properties such as short-range molecular order, bond lengths, bond angles, and the details of the phonon spectrum, may be preserved on the molecular scale and yet not be detected by the above techniques. Since Mössbauer spectra primarily reflect the local electronic environment of the probe nuclei, Mössbauer spectroscopy provides an excellent technique for studying the nature of the crystalline ordering on the atomic scale.

In the amorphous state of solids, some physical and chemical properties are substantially altered from those in the corresponding crystalline state. Crystal deformations are directly reflected in the Mössbauer parameters, namely, (i) the isomer shift is sensitive to the atomic valence states, bond angles, and atomic spacings; (ii) the quadrupole interaction depends on

the symmetry of the charge surrounding the probe nucleus; and (iii) the recoil-free fraction is a measure of various moments of the phonon spectrum.

The characterization of the amorphous state by the Mössbauer effect has been the subject of several studies,²⁻⁹ particularly in tin (¹¹⁹Sn) and chalcogenide (¹²⁵Te) glasses. In a study of amorphous and crystalline tellurium² it was observed that in the amorphous phase the quadrupole splitting is slightly increased and the recoil-free fraction is about one third as large as in the crystalline phase. These changes were attributed to a decrease in the length of the predominantly covalent bond and to the presence of broken dangling bonds. Metal-oxide bonds, on the other hand, are predominantly of ionic character. In studies of tin-oxide glasses of alkali, silicate,³ borate,⁴ and of more-complex materials,⁵ the influence of the constituents of the dopants on the Mössbauer parameters has been investigated. But up to now studies have not been conducted to characterize the glassy state of the pure metal-oxide system.

In the present work, we investigate the nature of a Sn-O amorphous system by combining the Mössbauer effect with electron microscopy and diffraction. In order to ensure a high degree of amorphism of the Sn-O system, the samples were prepared by the direct reaction of tin atoms with molecular oxygen. The results are compared with those obtained with polycrystalline SnO₂ and SnO (gray). As will be shown, the Mössbauer effect indeed displays changes in properties of the amorphous and crystalline states not revealed by electron microscopy and diffraction.

EXPERIMENTAL AND DATA ANALYSIS

Studies¹⁰ on the lattice dynamics of granular tin ($\langle d \rangle = 35 \text{ \AA}$) embedded in a tin-oxide matrix, and electron diffraction studies, showed that the oxide formed by evaporation of metallic tin in the presence of oxygen and condensation on a cold substrate may be characterized as amorphous. In the present studies a similar technique was employed to prepare absorbers. We report the results obtained for two amorphous samples prepared under similar conditions except for the tin evaporation rate.

Pure metallic tin (99.95%) was evaporated from a tantalum crucible in an evacuated chamber. O_2 was allowed into the chamber through a needle valve and the oxidation reaction took place in the gas while the resulting tin oxides were collected on the surface of an aluminum foil thermally anchored to a liquid nitrogen reservoir. A carbon grid necessary for electron microscopy was attached to this foil and a shutter was temporarily open to allow evaporation of a film approximately 800 \AA thick. The evaporation rate was controlled with a quartz-crystal thickness monitor and the O_2 pressure with an ion gauge. The oxygen pressure was kept in the range of $(0.5 \text{ to } 1) \times 10^{-3}$ Torr. The evaporation rate of the first sample (A) was $300 \text{ \AA}/\text{min}$ and of the second (B) $50 \text{ \AA}/\text{min}$. An electron microscope picture obtained with the film of sample B is shown in Fig. 1. Micro-



FIG. 1. Electron-microscope spectrum of sample B. The crystals appearing at the lower left of the photograph represent microcrystals of MgO of about 70 \AA in size mixed in the sample for calibration purposes.

crystals of MgO ($\langle d \rangle = 70 \text{ \AA}$) shown in this figure were used as reference and size calibration. No crystalline domains down to 25 \AA were observed in either sample A or B and no diffraction lines corresponding to the tin oxides could be detected either. However, weak and broad diffraction lines of β -Sn were observed in sample A which was prepared with higher Sn concentration. The absorbers used for

TABLE I. Mössbauer-spectra parameters at room temperature. Errors are statistical. The source: $CaSnO_3$ at room temperature. Isomer-shift scale assumes that the β -Sn- $CaSnO_3$ shift is the same as the β -Sn- $BaSnO_3$ shift.

Sample	Linewidth (FWHM) Γ (mm/sec)	Isomer shift δ (mm/sec)	Quadrupole splitting Δ (mm/sec)	Debye temperature Θ_{DW} (K)
$Sn^{4+}O_2$				
Amorphous (sample B)	1.04(1)	+0.129(3)	0.701(6)	243 ± 3
crystalline	0.965(16)	+0.004(3)	0.499(13)	313 ± 6
$Sn^{2+}O$				
Amorphous (sample B)	1.23(2)	+2.871(7)	1.71(2)	181 ± 2
crystalline (gray)	0.916(8)	+2.678(3)	1.36(1)	203 ± 1

$$R = \frac{\text{Intensity}(Sn^{2+})/f(Sn^{2+})}{\text{Intensity}(Sn^{4+})/f(Sn^{4+})}; R_A = 0.23, R_B = 0.82$$

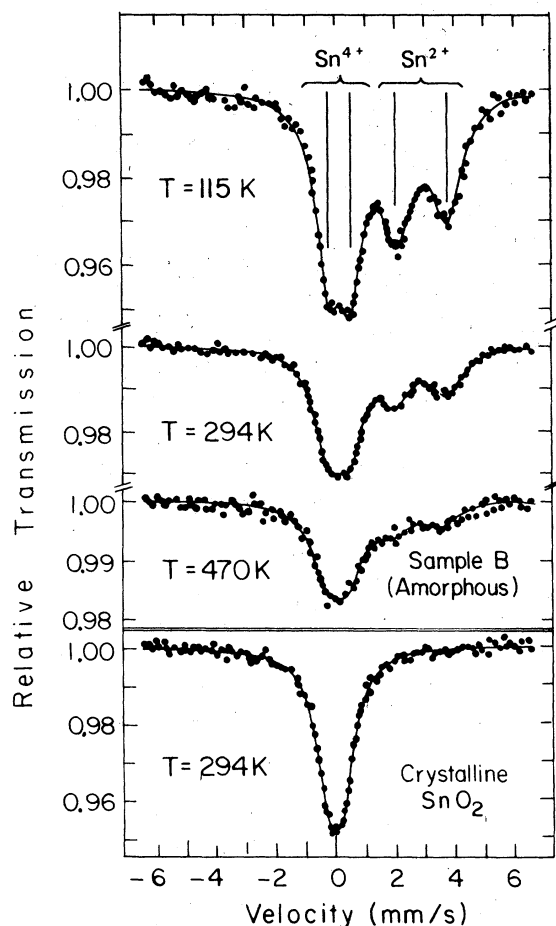


FIG. 2. Characteristic Mössbauer spectra obtained with sample B, and room-temperature spectrum of crystalline SnO_2 for comparison.

the Mössbauer spectroscopy were prepared by thoroughly mixing the oxide with Al_2O_3 powder and packing in an aluminum holder. Reference Mössbauer absorbers of high-purity polycrystalline SnO_2 and SnO (gray) were also prepared with thicknesses similar to those of the amorphous samples ($\sim 0.2 \text{ mg/cm}^2$ of ^{119}Sn).

A variable temperature cryostat operating in the range of 100–480 K was used for the Mössbauer spectroscopy. Sources of V-Sn alloy or of CaSnO_3 were kept at room temperature. The absorption spectra were analyzed by fitting to Lorentzian lines, using a least-squares-fitting program; the resulting spectral parameters for sample B and for the reference samples are given in Table I. Representative spectra of sample B are shown in Fig. 2. Lines characteristic of Sn^{2+} (SnO) and Sn^{4+} (SnO_2) are observed. A line attributed to $\beta\text{-Sn}$ on the basis of its isomer shift is also evident in the spectra obtained with sample A.

The temperature dependence of the area under the absorption lines of amorphous SnO and SnO_2 (sample B) and of the corresponding reference crystalline absorbers is shown in Fig. 3. The areas are normalized at 100 K. Because of the difficulties in characterizing the granularity of the samples, the areas were not corrected for saturation due to finite resonant thickness. But such corrections should be small for these thin ($n\sigma f = t < 1.5$) absorbers. The characteristic Debye temperature Θ_{DW} was derived from a least-squares fit to these areas based on a high-temperature approximation of the recoil-free fraction¹¹

$$\ln f = -6E_R T / k_B \Theta_{\text{DW}}^2 + E_R / 6k_B T,$$

where E_R is the recoil energy and k_B is the Boltzmann constant. The results for Θ_{DW} are given in Table I. From the relative intensities of the absorption lines, and the calculated recoil fraction f of each constituent, the ratio of Sn^{2+} to Sn^{4+} sites in each sample was determined. These results are also given in Table I.

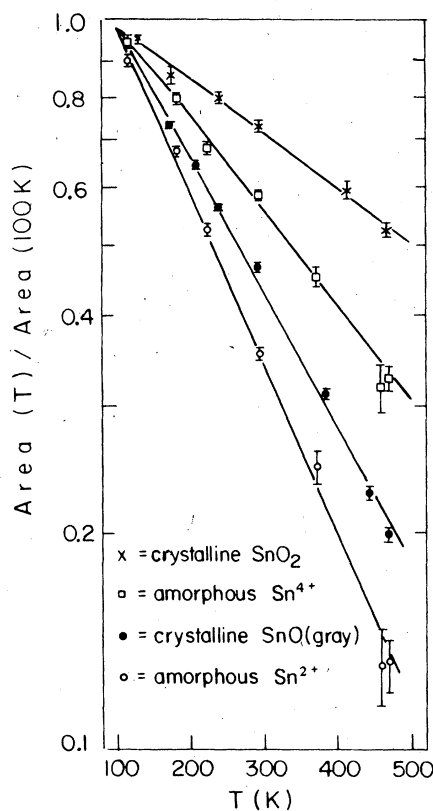


FIG. 3. Temperature dependence of the area under the resonance lines obtained with crystalline and amorphous SnO_2 and SnO absorbers.

The temperature dependence of the isomer shift was consistent with that calculated from the second order Doppler shift for a sample at constant volume. A detailed analysis of the explicit temperature dependence of the isomer shift was not performed because the coefficients of thermal expansion are not known for these samples.

DISCUSSION

Although samples A and B were characterized as amorphous by electron diffraction, the Mössbauer measurements indicate that they are dissimilar. Sample A has recoil-free fractions, isomer shifts, and quadrupole splittings close to those of the polycrystalline oxides. But this is not the case for sample B. The conditions under which sample B was prepared, namely, low evaporation rate of metallic tin, produce comparatively large changes in the Mössbauer parameters: the degree of amorphism is clearly greater in sample B.

Now we concentrate on results obtained with samples B and try to characterize its structure relying solely on the Mössbauer-effect data. Both Sn^{2+} and Sn^{4+} states are observed. The quadrupole splitting and isomer shift values of these states are of the same order of magnitude as those for the crystalline SnO_2 and gray SnO , but different enough to suggest that the immediate environment of the amorphous Sn^{2+} and Sn^{4+} can be described as a distorted crystalline cell. The crystal structure¹² of SnO_2 is of the rutile type; the Sn^{4+} is situated in a distorted octahedron, all Sn-O distances are equal in the basal plane, yet the O-Sn-O angles are not 90° but 78° and 102° , respectively. The Sn-O axial distance in the direction perpendicular to the basal plane are longer by 2% than those in the base. Such a structure will produce a non-axially-symmetric electric field gradient.

The quadrupole splitting Δ is given by

$$\Delta = \frac{1}{2}(e^2qQ)\left(1 + \frac{1}{3}\eta^2\right)^{1/2},$$

where q is the electric field gradient, Q is the ^{119}Sn quadrupole moment, and η is the asymmetry parameter. For $0 < \eta < 1$, Δ can not vary by more than 15% through a change in the symmetry alone: hence the large change in the quadrupole splittings between the amorphous and crystalline samples must be attributed to a further elongation of the axial Sn-O bond with respect to the basal bonds rather than to an angular rearrangement of the basal bonds themselves. The bonding is predominantly produced by sp^3 hybridized orbitals. The isomer shift of the amorphous Sn^{4+}O is more positive (by 0.12 mm/sec) than in the crystalline case, suggesting a larger s density at the nucleus. This trend is consistent with the hypothesis of larger interatomic distances in the amorphous sam-

ple: the oxygen removes fewer electrons from the Sn ions.

The crystal structure of gray SnO is tetragonal,¹³ Sn^{2+} sits at the top of a square pyramid. Here the main contribution to the electric field gradient arises from the unbalanced p electron population. As in the case of Sn^{4+} , both the isomer shift and the quadrupole splitting increase in the amorphous material. The increase of the electric field gradient can be attributed to an increase in the difference between the p -electron population in the z direction and the population in the x - y plane ($\sigma_p - \pi_p$) compatible with an axial elongation of the pyramid. Thus, the general interpretation of the hyperfine interaction for both Sn^{2+} and Sn^{4+} sites is that the axial Sn-O bond length is larger in the amorphous state.

Both the Sn^{2+} and Sn^{4+} sites exhibit relatively narrow lines and both have essentially the same relative broadening

$$(\Gamma_{\text{amorph}} - \Gamma_{\text{cryst}})/\Delta \approx 0.16$$

suggesting a narrow distribution of electric field gradients for both sites. Furthermore, the electric field gradients in the amorphous and crystalline samples are quite different from each other and their distributions do not overlap; that is, the spectra of the amorphous sample contain virtually no components characteristic of the normal crystalline state. This indicates that amorphism down to the atomic scale extends throughout the entire sample.

The slope of $\ln f(T)$ at high temperatures ($T > \Theta_D/2\pi$) is proportional to Θ_{DW} , the (-2) moment of the phonon spectrum. Whereas the isomer shift and quadrupole splitting are better measures of the nearest neighbor distortion, Θ_{DW} rather reflects bulk properties. For sample A, Θ_{DW} did not change appreciably: there is only a 5% reduction in Θ_{DW} for the Sn^{4+} component, and 3% reduction in Θ_{DW} for the Sn^{2+} component. This result suggests fairly long range crystalline order but with an upper limit of 25 Å indicated by the electron micrograph. For sample B, however, Θ_{DW} decreases markedly with respect to Θ_{DW} of the crystal, by as much as 22% and 11% for the Sn^{4+} and Sn^{2+} components, respectively, indicating a significant increase in the population of soft phonons in the phonon spectrum of the amorphous tin oxide. This result is consistent with our picture of the elongation of the Sn-O bond in the amorphous material. It also supports the interpretation of atomic scale amorphism. With this conclusion in mind, we envisage an amorphous SnO system composed of units of distorted octahedra with central Sn^{4+} linked by Sn-O bonds, where bridging Sn^{2+} lie on the apex of a pyramid with an approximate Sn^{2+} -to- Sn^{4+} site occupation ratio of ≈ 0.8 .

Finally we conclude that when the oxidation reaction of the $\text{Sn} + \text{O}_2$ takes place in a medium of fast

freezing of the reactants, both Sn^{4+} and Sn^{2+} valence states are formed, where the $2+$ state is perhaps a frozen intermediate state toward the fully oxidized Sn^{4+} . This speculation is also supported by additional results obtained with a sample condensed on a room temperature substrate: some metallic β -Sn but virtually no Sn^{2+}O could be seen in the Mössbauer spectra.

It should be mentioned that we do not suggest that sample B shows the maximum degree of amorphism of tin oxide. Systematic studies of the influence of substrate temperature and of the Sn-O₂ concentration

on the amorphous properties as observed by Mössbauer spectroscopy might achieve a higher degree of disorder in the Sn-O system.

Nevertheless, the results show that Mössbauer spectroscopy is a powerful tool for identifying on the atomic scale residual crystalline properties of materials otherwise characterized as amorphous.

ACKNOWLEDGMENT

This work was supported by the NSF.

*Present address: Dept. of Physics, Clark University, Worcester, Mass.

¹J. M. D. Coey, *J. Phys. (Paris) Suppl.* **12**, C6-89 (1974).

²N. A. Blum and C. Feldman, *Solid State Commun.* **15**, 965 (1974).

³G. M. Bartener, S. M. Brekhovskikh, A. Z. Varisov, L. M. Landa, and A. D. Tsyganov, *Sov. Phys. Solid State* **12**, 972 (1970).

⁴K. P. Mitrofanov and T. A. Sidorov, *Sov. Phys. Solid State* **9**, 963 (1967).

⁵G. M. Bartenev, V. A. Gorokhovskii, A. D. Tsyganov, V. P. Scherbakova, and A. I. Ouchinnikov, *Inorg. Mater.* **8**, 1934 (1972).

⁶P. P. Seregin, Yu. V. Kryl'nikov, F. S. Nasrebinov, L. N.

Vasil'ev, M. A. Sagatov, and E. Yu. Turaev, *JETP Lett.* **20**, 57 (1974).

⁷J. Bolz and F. Pobell, *Z. Phys. B* **20**, 95 (1975).

⁸P. Boolchand, B. B. Triplett, S. S. Hanna, and J. P. de Neufville, *Mössbauer Effect Methodology* (Plenum, New York, 1974), Vol. 6, p. 53.

⁹P. Boolchand, M. Tenhover, and R. E. Flasck, *AIP Conf. Proc.* **31**, 102 (1976).

¹⁰S. Akselrod, M. Pasternak, and S. Bukshpan, *Phys. Rev. B* **11**, 1040 (1975).

¹¹R. M. Housley and F. Hess, *Phys. Rev.* **146**, 517 (1966).

¹²W. H. Baur, *Acta Crystallogr.* **2**, 515 (1956).

¹³R. W. G. Wyckoff, *Crystal Structure* (Interscience, New York, 1965), Vol. I, pp. 134-136.



FIG. 1. Electron-microscope spectrum of sample B. The crystals appearing at the lower left of the photograph represent microcrystals of MgO of about 70 Å in size mixed in the sample for calibration purposes.